

Spin-blockade effect and coherent control of DNA-damage by free radicals: a proposal on bio-spintronics

Ramin M. Abolfath^{1,2}, Thomas Brabec¹

¹*Physics Department, University of Ottawa, Ottawa, ON, K1N 6N5, Canada*

²*School of Natural Sciences and Mathematics, University of Texas at Dallas, Richardson, TX 75080*

(Dated: November 10, 2018)

Coherent control of OH-free radicals interacting with the spin-triplet state of a DNA molecule is investigated. A model Hamiltonian for molecular spin singlet-triplet resonance is developed. We illustrate that the spin-triplet state in DNA molecules can be efficiently populated, as the spin-injection rate can be tuned to be orders of magnitudes greater than the decay rate due to small spin-orbit coupling in organic molecules. Owing to the nano-second life-time of OH free radicals, a non-equilibrium free energy barrier induced by the injected spin triplet state that lasts approximately longer than one-micro second in room temperature can efficiently block the initial Hydrogen abstraction and DNA damage. For a direct demonstration of the spin-blockade effect, a molecular simulation based on an *ab-initio* Car-Parrinello molecular dynamics is deployed.

Organic molecules including DNA have been proposed to be used in electronic circuits as molecular conductors and nanowires [1]. They are attractive alternatives to inorganic semiconductors for a variety of optoelectronic devices, e.g. photovoltaics. Their long spin lifetime [2] can make them desirable for applications in spintronics [3]. The unique biological functionality of DNA-molecules in carrying the genetic information can be used for *bio-spintronics*.

We investigate here the possibility to couple coherent control methods [4] with bio-spintronics. OH-free radicals that are products of chemical reactions or ionizing radiation [5] are highly reactive and toxic, resulting in DNA-damage (single/double strand break), and the development of genetic aberrations, carcinogenesis and aging. They are highly unstable diatomic molecules with a life-time that is reported within nano-seconds and are charged neutral with a magnetic moment that is produced by nine electrons with an unpaired spin in the outermost open shell. Their high reactivity is thus attributed to the pairing of opposite spin electrons in the open orbital of the free radical with an electron in an organic molecule. Fenton chemistry studies used in nucleic acid foot-printing show that a free radical reaches a DNA-molecule by diffusion and removes a hydrogen ion from its sugar moiety (e.g., a deoxyribose) [6–8]. The most probable sites of attack are identified as H_{5'}, H_{5''}, and H_{4'} of the deoxyribose residue in the backbone of the DNA (the nomenclature is adopted following Ref. [8]). Because of their short life-time of 1 ns, OH radicals generated within 1 nm from the surface of the DNA molecule can remove a hydrogen ion and form a water molecule.

We show here that by optical pumping the HOMO electron of both, the OH-free radicals and the DNA, can be efficiently spin-polarized. Paramagnetic state of OH-radical can be oriented along the non-equilibrium direction of the triplet magnetic moment of the DNA molecule. Such photo-excited DNA follow a phosphorescence decay to the ground state with slow transition rate,

hence providing statistically enough triplet excitons to block OH-DNA reactivity. The reported triplet life-time of DNA nucleotides ranges 1 μ s at room temperature to 1s at 77K [2]. The Hydrogen abstraction occurs in 1 ps, several order of magnitudes faster than the DNA triplet decay process. The disparity in time scale between the chemical reaction and DNA-triplet life-time allow us to use a ps Car-Parrinello *ab-initio* molecular dynamics to simulate the immunization of DNA against OH-free radicals.

Recent studies in pump and probe femto-second laser spectroscopy of nucleic-acids in solutions have provided valuable information on the optical excitations of nucleotides and their decay pathways to the ground state through radiative and non-radiative channels [9–12]. These studies have identified the spin multiplicities of the excited states including their life-times and quantum yields. As shown in Fig. 1 the major photo-excitation of all bases of nucleic-acids occur close to the wavelength $\lambda = 260$ nm (UV) where a direct transition from singlet ground state S_0 to singlet excited state $^1\pi\pi^*$ is observed. Unlike III-V/II-VI semiconductors that strong SO-coupling has led to direct observation of the optical spin excitations in which a laser generates a population of photo-carriers strongly spin polarized along a direction which depends on the polarization state of the laser field [16], in organic molecules no direct optical transition to spin triplet state has been reported. However, the emission spectrum governed by inter-system crossing and SO coupling has revealed the spin triplet states, $^3\pi\pi^*$, with energy below $^1\pi\pi^*$. Consistent with the emission spectrum, our *ab-initio* calculation shows that the lowest energy singlet-triplet energy gap (Δ_X) of DNA-bases and DNA-backbone are close to 2.68 eV (corresponding to $\lambda = 463$ nm) for DNA-base, and 2.38 eV ($\lambda = 521$ nm) for sugar moiety.

We employ a model Hamiltonian consisting of four HOMO-LUMO molecular levels as shown in Figure 1. The figure shows schematically the direct photo-induced

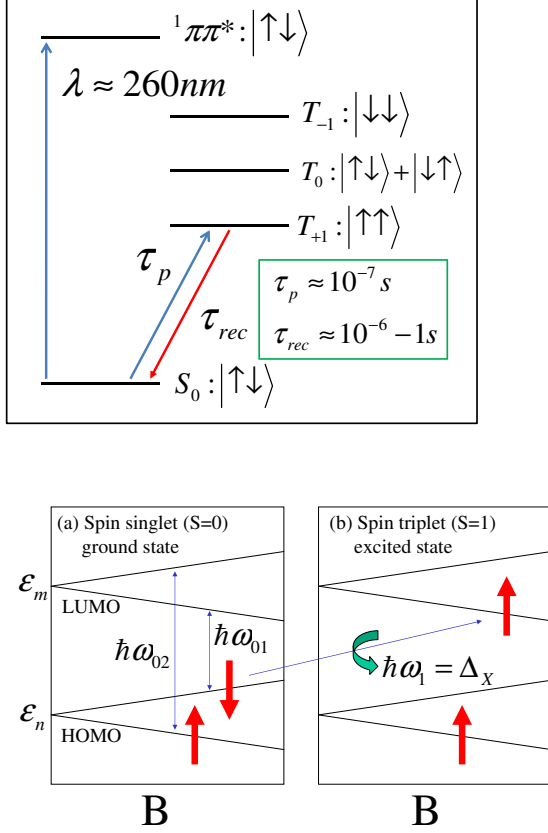


FIG. 1: Schematically shows the typical energy level diagram (top) and the direct transition of spin singlet-triplet resonance (bottom) in the presence of external magnetic field.

spin singlet-triplet transitions ($S = 0 \rightarrow 1$). The molecular levels shown in Figure 1 represent the ground and excited states of the DNA-molecule. In the absence of an external magnetic field, the electronic ground state of the DNA-molecule is $S = 0$ spin-singlet with double occupancy of the molecular orbitals. The two-fold degeneracy of the molecular orbitals is lifted by a weak magnetic field that couples to the electron spin through the Zeeman interaction [15], $E_Z = g\mu_B \vec{S} \cdot \vec{B}$. Here E_Z is the Zeeman energy, g is the electron g -factor ($g \approx 2$), μ_B is the Bohr magneton ($\mu_B \approx 5.8 \times 10^{-5}$ eV/Tesla), and B is the strength of the external magnetic field along quantization axis, \hat{z} .

In the Born-Oppenheimer approximation, the $S = 1$ spin-flip excitation is constructed by removing an electron from an occupied S_0 state and putting into an unoccupied state with opposite spin. By denoting quasi-particle energy levels (electron dressed by interaction) by $\varepsilon_{n\sigma} = \varepsilon_n + \Sigma(n, \sigma)$, the energy of one exciton is $\Delta_X = \varepsilon_{m\uparrow} - \varepsilon_{n\downarrow} - \langle m \uparrow, n \downarrow | V | n \downarrow, m \uparrow \rangle$. Here the indices n

and m label HOMO and LUMO, and $\sigma = +1, -1$ is used for spin up and down. ε_n is the n th single particle molecular energy level, $\Sigma(n, \sigma) = \sum_{n' \in \text{occ.}} [2\langle n, n' | V | n', n \rangle - \langle n, n' | V | n, n' \rangle]$ is the electron self-energy and summation has carried out over all occupied orbitals, V is the electron-electron repulsive Coulomb interaction, and $\Delta_X = E_{\text{triplet}} - E_{\text{singlet}}$ is the energy of an exciton relative to the S_0 ground state energy. An intra-molecular transition accompanied with electron spin flip, can be achieved by application of an inhomogeneous perpendicular magnetic field $\vec{B}_\perp = B_\perp(\vec{r})(\hat{x} \cos \omega_1 t - \hat{y} \sin \omega_1 t)$, assuming $\omega_1 > 0$. The quasi-particle energy levels shown in Fig. 1, form a 4×4 block-diagonal Hamiltonian, H . It can be decomposed to two 2×2 Hamiltonians H_1 and H_2 , i.e., $H = H_1 \oplus H_2$. Here $H_1 = H_1^{(0)} + H_1^\perp$ is the two level Hamiltonian with the basis $|n \downarrow\rangle$, and $|m \uparrow\rangle$ that form the diagonal matrix $H_1^{(0)} = \varepsilon_{n\downarrow}|n \downarrow\rangle\langle n \downarrow| + \varepsilon_{m\uparrow}|m \uparrow\rangle\langle m \uparrow|$ with $\varepsilon_{n\sigma} = \varepsilon_n - \sigma \frac{\hbar\gamma}{2} B$. Here $\gamma = g\mu_B/\hbar$ is the electron gyromagnetic ratio, and the HOMO-LUMO single particle energy gap is $\hbar\omega_{01} = \varepsilon_{m\uparrow} - \varepsilon_{n\downarrow} = (\varepsilon_m - \varepsilon_n) - \hbar\gamma B$. Application of $\vec{B}_\perp(\vec{r}, t)$ allows a direct transition from spin down to spin up (as shown in Figure 1). The Hamiltonian that describes the coupling of the molecular orbitals with in-plane magnetic field can be expressed as $H_1^\perp = -\frac{1}{2}\hbar\gamma B_\perp^{nm} [\exp(i\omega_1 t)|n \downarrow\rangle\langle m \uparrow| + \exp(-i\omega_1 t)|m \uparrow\rangle\langle n \downarrow|]$. Here $B_\perp^{nm} = \langle n | B_\perp(\vec{r}) | m \rangle$ is the off-diagonal matrix element of inhomogeneous in-plane magnetic field that allows mixing of HOMO and LUMO. Finally

$$H_1 = \begin{pmatrix} \varepsilon_{n\downarrow} & \Delta \exp(i\omega_1 t) \\ \Delta^* \exp(-i\omega_1 t) & \varepsilon_{m\uparrow} \end{pmatrix}, \quad (1)$$

where $\Delta = -\hbar\gamma B_\perp^{nm}/2$. Similarly

$$H_2 = \begin{pmatrix} \varepsilon_{n\uparrow} & \Delta \exp(-i\omega_1 t) \\ \Delta^* \exp(i\omega_1 t) & \varepsilon_{m\downarrow} \end{pmatrix}. \quad (2)$$

In H_2 the quasi particle energy gap is $\hbar\omega_{02} = \varepsilon_{m\downarrow} - \varepsilon_{n\uparrow} = (\varepsilon_m - \varepsilon_n) + \hbar\gamma B$. Note that the oscillating in-plane magnetic field in H_1 provides the spin-flip resonance with the transition probability given by $P_{n\downarrow \rightarrow m\uparrow} = (|\Delta/\hbar|^2/\Omega_R^2) \sin^2(\Omega_R t/2)$. Here $\Omega_R = \sqrt{(\omega_{01} - \omega_1)^2 + |\Delta/\hbar|^2}$. Note that $\Omega_R = \Delta/\hbar$ is the corresponding Rabi frequency at the resonance $\omega_{01} = \omega_1$ where the optical HOMO-LUMO transition accompany with the spin flip-flop shows the highest probability. In the last equality we ignored electron-hole Coulomb attraction. Inclusion of V is expected to shift the predicted resonance peak to $\omega_1 = \Delta_X/\hbar$. In contrast, because of negative sign of ω_1 in H_2 , the oscillating in-plane magnetic field does not make a resonance between opposite spins in HOMO and LUMO. Therefore the spin flip transition induced by B_\perp occurs only between $|n \downarrow\rangle$ and $|m \uparrow\rangle$, in accordance with angular momentum conservation law. The transition time for spin singlet to triplet of a π -pulse can be calculated by $\tau_p = (2\pi/g)(mc^2/e\mathcal{E}_\perp)/c$ where $\mathcal{E}_\perp = c\sqrt{\langle B_\perp^2 \rangle}$. The

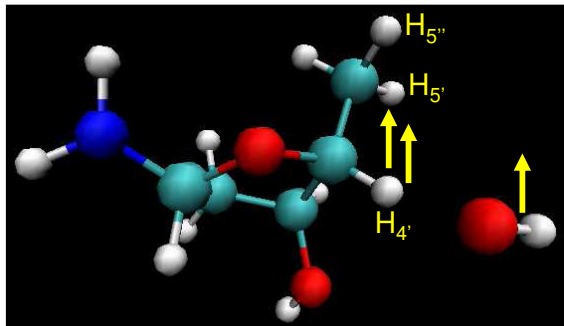


FIG. 2: Initial state of deoxyribose molecule in the presence of OH free radical. Schematically shown the injection of photo-generated electrons in deoxyribose with spin polarization (shown by arrows) along the direction of circularly polarized light and external magnetic field. The net magnetic force between two parallel magnetic moments localized in OH and deoxyribose is repulsive. This is similar to two separated magnetic moments which interact like Heisenberg antiferromagnetic exchange coupling.

steady state population of spin-triplet state n_T can be calculated by $n_T = n_0\tau_r/(\tau_r + \tau_p)$ where n_0 is the density of the DNA-base in solution or on the surface-density of DNA-bases on the chromatin in nucleus of the cell accessible to the solvent (free radicals). As $\tau_r \gg \tau_p$, the optically pumped spin-triplet state quickly saturates. A laser field with intensity of $1\text{W}/\text{mm}^2$ is technologically achievable that gives $\tau_p \approx 10^{-7}\text{s}$.

Figure 2 schematically shows optically excited electron-hole pair (exciton) in the DNA-backbone in the presence of spin-polarized OH free radical. Because the absorption of a photon alters the local electronic state of a DNA-molecule, we confine our simulation to a particular segment, e.g., only a part of DNA where the injected exciton is presumably localized and the optical transition takes place, e.g., close to the site of attack. Our DNA-backbone model is similar to the deoxyribose residue used in other *ab-initio* calculation such as Ref. [13] where the system of interest consists of a DNA nucleobase modeled by an amino group attached to the deoxyribose in the presence of the OH-radical as shown in Figure 2. We selectively choose the site of OH-radical attack in the vicinity of $\text{H}_{5'}$, $\text{H}_{5''}$, and $\text{H}_{4'}$ of deoxyribose residue in the back-bone of DNA because of the accessibility of these sites to the solvent [6–8]. Following Ref. [14] we identify the dehydrogenation of the deoxyribose as a function of spin multiplicity. The ground and excited states of the deoxyribose correspond to spin sin-

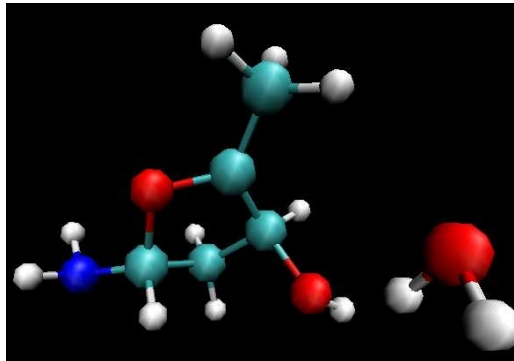


FIG. 3: The state of de-hydrogenated deoxyribose by OH free radical at $t = 0.15$ ps (a few time-steps after initial hydrogen abstraction). In this simulation $\text{H}_{4'}$ on deoxyribose is abstracted. The polarization state of the system is spin doublet ($S = 1/2$).

glet ($S = 0$), and spin triplet ($S = 1$) states. As the life time of both spin-polarized OH radical and spin-triplet exciton in DNA-backbone is much longer than the simulation time, we perform CPMD [18] calculation under restricted spin configuration. We choose two classes of spin-restricted calculations, as the total spin along the quantum axis is subjected to the constraints $S_z = 1/2$, and $3/2$, corresponding to doublet and quartet spin configurations. In both calculations the initial distance between OH-radical and DNA-backbone is considered to be approximately 1.5 \AA .

The initial and final states of the molecules are shown in Figures 2-4. The final configurations of the molecules have been obtained after 0.6 ps where the rearrangement of the atomic coordinates have been deduced from a dynamical trajectory calculated by CPMD. According to our results, a dehydrogenation of the deoxyribose takes place around 0.15 ps for a system with $S_z = 1/2$ (total spin-doublet) as shown in Figure 3. This process leads to the formation of a water molecule, and $\text{H}_{4'}$ turns out to be the site of Hydrogen abstraction in this simulation. In contrast, as shown in Figure 4, in the quartet spin configuration the repulsive exchange interaction blocks the exchange of hydrogen and hence the chemi-

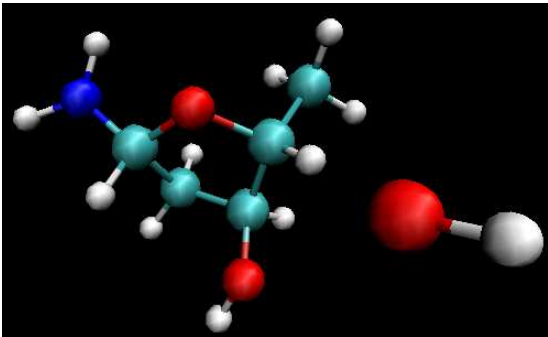


FIG. 4: The state of radio-resistive deoxyribose at $t = 0.6$ ps. The polarization state of the system is spin quartet ($S = 3/2$) induced by circularly polarized light in the presence of weak magnetic field. Due to injected localized and polarized photoelectrons, the dehydrogenation of DNA-backbone does not occur.

cal reaction. To systematically check the convergence of the results, we increased the size of the DNA-molecule by adding phosphates and nucleotides and constructed a double strand DNA. We used a quantum mechanical (QM) approach to simulate the Hydrogen abstraction in a small segment of DNA molecule and molecular mechanics (MM) approach to simulate the vibrational modes of the rest of molecule [19], and found no influence on the spin-blocking effect. The details of this study will be presented elsewhere. To estimate the energy needed for the polarization of the deoxyribose in the absence of OH-radicals, we calculated the energy of the ground and excited states of the gas-phase deoxyribose in spin singlet and triplet multiplicities with the spin singlet-triplet energy gap $\Delta_X \approx 2.38$ eV. This provides an estimate for the frequency of the optical gap shown in Figure 1, which is within the range of the visible spectrum of the electromagnetic waves, $\lambda = 521$ nm, corresponding to green

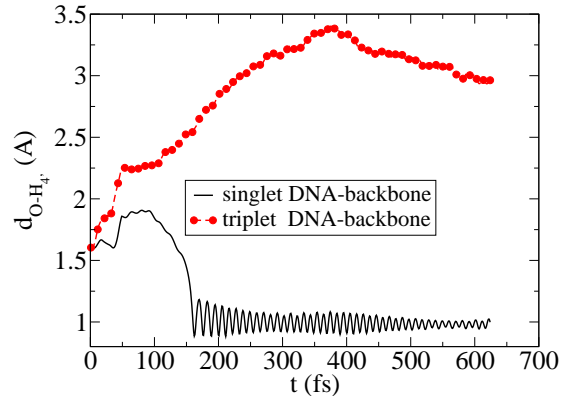


FIG. 5: Evolution of the separation of oxygen atom in OH radical with respect to $H_{4'}$ in deoxyribose. The dependence on the spin multiplicity is seen. The hydrogen abstraction occurs approximately at $t = 150$ fs in the spin singlet state of deoxyribose. The process of initial damage to DNA-backbone is blocked in deoxyribose due to excessive spin with direction parallel to the spin polarization of OH free radical.

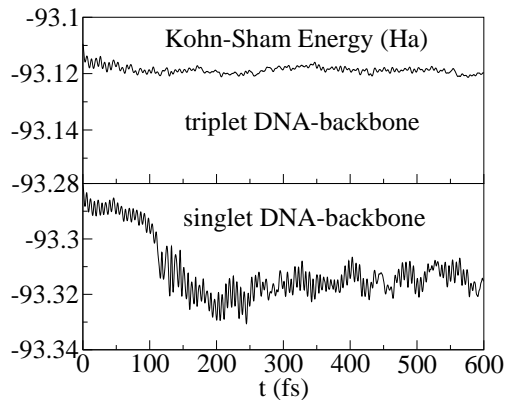


FIG. 6: Kohn-Sham energy as a function of time and spin-multiplicity of deoxyribose. An almost flat Kohn-Sham energy of spin triplet state of deoxyribose (top) is indication of the repulsive interaction between magnetic moments of OH free radical and $S = 1$ exciton due to spin-blockade effect. In contrast, a drop in Kohn-Sham energy of spin singlet state of deoxyribose (bottom) indicates that the dehydrogenation of $H_{4'}$ occurs approximately at $t = 150$ fs.

light. To estimate the stored magnetic energy due to the optical injection of spin, we calculated the energy of the gas-phase deoxyribose in the presence of one OH-free radical with spin doublet and quartet multiplicities. For the molecules shown in Figure 2, we find the energy gap $\tilde{\Delta}_X \equiv E_{\text{quartet}} - E_{\text{doublet}} \approx 3.05$ eV. Here the excessive magnetic energy which originated from spin-spin repul-

sive interactions (which resemble the anti-ferromagnetic exchange interaction in the Heisenberg model) can be deduced to be $\hat{\Delta}_X - \Delta_X \approx 0.67$ eV. This energy can be interpreted as the excessive energy barrier due to the alignment of the spins in deoxyribose and OH, and is the source of the magnetic repulsive force which makes the diffusion of OH toward DNA-backbone less likely. This is in agreement with the results obtained from CPMD. The distance between the oxygen atom in OH radical and H_{4'} in deoxyribose as a function of time and the spin multiplicity of deoxyribose is shown in Figure 5. A drop in Kohn-Sham energy seen in spin singlet state that is the indication of deoxyribose dehydrogenation, disappears in case of spin triplet state. Accordingly dehydrogenation of H_{4'} occurs approximately at $t = 150$ fs. The corresponding Kohn-Sham energies are shown in Figure 6. In spin triplet state of deoxyribose the spin-blockade effect is strong enough that it repels OH free radical.

In conclusion, we have examined spin-blockade mechanism to propose coherent control of DNA-OH interaction, in particular from the initial damage induced by OH free radicals. To achieve an efficient direct pumping of triplet states from the singlet ground state we illustrated that the photo-excitation pumping rate can be tuned to be faster than the reported phosphorescence lifetime, however, an indirect transition via $S_0 \rightarrow {}^1\pi\pi^* \rightarrow {}^3\pi\pi^*$ is an alternative optical pumping pathway that can be used. The model calculation was performed using ab-initio Car-Parrinello molecular dynamics of a deoxyribose residue attached to amino-group in the presence of OH free radicals. We provided a detailed description of an experimental set up for spin-blockade detection.

[1] *Charge Migration in DNA*, Ed. T. Chakraborty (Springer-Verlag, Berlin, 2007).
 [2] H. Görner, J. Photochem. Photobiol. B **5**, 359 (1990); J. Photochem. Photobiol. B: Biology **26**, 117 (1994); C. Salet and R. Bensasson, Photochem. Photobiol. **22**, 231

(1975).
 [3] I. Žutić, J. Fabian, and S. Das Sarma, Rev. Mod. Phys. **76**, 323 (2004).
 [4] H. Rabitz, R. de Vivie-Riedle, M. Motzkus, and K. Kompa, Science **288** 824 (2000).
 [5] Eric J. Hall, *Radiobiology for the Radiologist*, (Lippincott Williams & Wilkins, Baltimore, Fifth Edition, 2000); D. Becker, A. Adhikary, and M. Sevilla in *Charge Migration in DNA*, Ed. T. Chakraborty (Springer-Verlag, Berlin, 2007).
 [6] B. Balasubramanian, W. K. Pogożelski, and T. D. Tullius, Proc. Natl. Acad. Sci. **95**, 9738 (1998).
 [7] T. D. Tullius and J. A. Greenbaum, Current Opinion in Chemical Biology **9**, 127 (2005).
 [8] W. K. Pogożelski and T. D. Tullius, Chem. Rev. **98**, 1089 (1998); C. J. Burrows, and J. G. Muller, Chem. Rev. **98**, 1109 (1998).
 [9] Chris T. Middleton, Kimberly de La Harpe, Charlene Su, Yu Kay Law, Carlos E. Crespo-Hernandez, and Bern Kohler, Annu. Rev. Phys. Chem. **217** (2009).
 [10] Juan Jose Serrano-Perez, Remedios Gonzalez-Luque, Manuela Merchan, and Luis Serrano-Andres, J. Phys. Chem. B. **111**, 11880 (2007).
 [11] Manuela Mercha, Luis Serrano-Andre, Michael A. Robb, and L. Blancafort, J. AM. CHEM. SOC. **127**, 1820 (2005).
 [12] Patrick M. Hare, Carlos E. Crespo-Hernandez, and Bern Kohler, J. Phys. Chem. B **110**, 18641 (2006).
 [13] K. Miaskiewicz and R. Osman, J. Am. Chem. Soc. **116**, 232 (1994).
 [14] Ramin M. Abolfath, J. Phys. Chem. B, **113**, 6938 (2009).
 [15] L. D. Landau, and E. M. Lifshitz, *Quantum Mechanics: Non-Relativistic Theory* (Pergamon, Oxford, 2003).
 [16] *Optical Orientation*, edited by F. Meier and B. P. Zakharchenya (North Holland, New York, 1984).
 [17] C. J. Mundy, M. E. Colvin, A. A. Quong, J. Phys. Chem. A. **106** 10063 (2002); Y. Wu, C. J. Mundy, M. E. Colvin, R. Car, J. Phys. Chem. A. **108** 2922 (2004).
 [18] J. Hutter, P. Ballone, M. Bernasconi, P. Focher, E. Fois, S. Goedecker, M. Parrinello, M. E. Tuckerman, *CPMD code, version 3.13*, MPI fuer Festkoerperforschung, Stuttgart IBM Zurich Research Laboratory, 1990-2008.
 [19] F. L. Gervasio, A. Laio, M. Iannuzzi, and M. Parrinello, Chem. Eur. J. **10**, 4846 (2004).